

Communication

Role of Halogen Substituents on Halogen Bonding in 4,5-DiBromohexahydro-3a,6-Epoxyisoindol-1(4H)-ones

Atash V. Gurbanov ^{1,2,*}, Dmitriy F. Mertsalov ³, Fedor I. Zubkov ³, Maryana A. Nadirova ³, Eugeniya V. Nikitina ³, Hieu H. Truong ^{4,*}, Mikhail S. Grigoriev ⁵, Vladimir P. Zaytsev ³, Kamran T. Mahmudov ^{1,2} and Armando J. L. Pombeiro ^{1,3}

¹ Centro de Química Estrutural, Instituto Superior Técnico, Universidade de Lisboa, Av. Rovisco Pais, 1049-001 Lisbon, Portugal; kamran.mahmudov@tecnico.ulisboa.pt (K.T.M.); pombeiro@tecnico.ulisboa.pt (A.J.L.P.)

² Department of Chemistry, Baku State University, Z. Khalilov Str. 23, Baku 1148, Azerbaijan

³ Organic Chemistry Department, Peoples' Friendship University of Russia (RUDN University), 6 Miklukho-Maklaya St, 117198 Moscow, Russia; keithred@mail.ru (D.F.M.); fzubkov@sci.pfu.edu.ru (F.I.Z.); mariannanadirova17@yandex.ru (M.A.N.); enikitina@sci.pfu.edu.ru (E.V.N.); vzaitsev@sci.pfu.edu.ru (V.P.Z.)

⁴ Institute of Research and Development, Duy Tan University, Danang 550000, Vietnam

⁵ Frumkin Institute of Physical Chemistry and Electrochemistry, Russian Academy of Sciences, Leninsky Pr. 31, Bld. 4, 119071 Moscow, Russia; mickgrig@mail.ru

* Correspondence: organik10@hotmail.com (A.V.G.); truonghonghieu@duytan.edu.vn (H.H.T.)



Citation: Gurbanov, A.V.; Mertsalov, D.F.; Zubkov, F.I.; Nadirova, M.A.; Nikitina, E.V.; Truong, H.H.; Grigoriev, M.S.; Zaytsev, V.P.; Mahmudov, K.T.; Pombeiro, A.J.L. Role of Halogen Substituents on Halogen Bonding in 4,5-DiBromohexahydro-3a,6-Epoxyisoindol-1(4H)-ones. *Crystals* **2021**, *11*, 112. <https://doi.org/10.3390/crust11020112>

Academic Editor: Marta E. G. Mosquera

Received: 3 January 2021

Accepted: 23 January 2021

Published: 26 January 2021

Publisher's Note: MDPI stays neutral with regard to jurisdictional claims in published maps and institutional affiliations.



Copyright: © 2021 by the authors. Licensee MDPI, Basel, Switzerland. This article is an open access article distributed under the terms and conditions of the Creative Commons Attribution (CC BY) license (<https://creativecommons.org/licenses/by/4.0/>).

1. Introduction

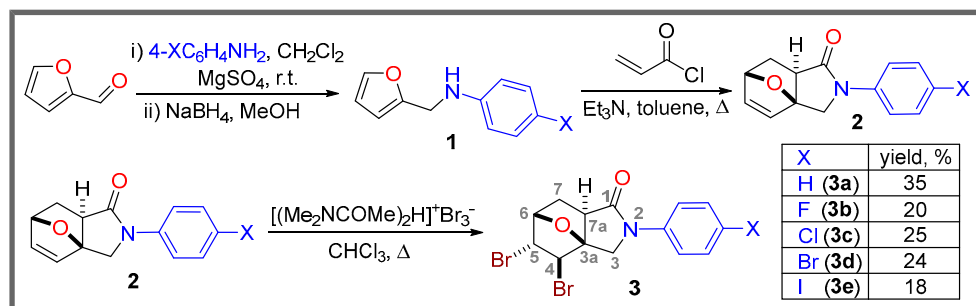
Halogen bonding ($R-Ha \cdots Nu$) is an important intermolecular interaction for the control and improvement of functional properties of materials [1–12]. The strength of halogen bonding $Ha \cdots Nu$ increases in the order $F \ll Cl < Br < I$ (with the increase of the polarizability of Ha) and with the electron-withdrawing character of R , as well as with the nucleophilicity of Nu at $R-Ha \cdots Nu$ [4]. The directionality of halogen bonding is much higher than that of the hydrogen bonding, and is dependent on R , Ha , and Nu [4]. In view of the high directionality and other bonding parameters (tunability, hydrophobicity, and donor atom dimensions), the halogen bonds have become a useful tool in synthesis, catalysis, crystal engineering, drug design, molecular recognition, material chemistry, etc. [1–13]. Thus, a variety of $Ha \cdots Ha$, $Ha \cdots Ch$ ($Ch =$ chalcogen), $Ha \cdots Pn$ ($Pn =$ pnictogen), $Ha \cdots \pi$ or $Ha \cdots$ anion synthons have been found in organic and coordination compounds [14]. Among them, the $Br \cdots Ha$ type of halogen bonding is a promising tool for controllable building of supramolecular architectures with predetermined structures and functional properties [2,4,15–18].

In particular, the effect of R on the halogen bonding at $R-Ha \cdots Nu$ has been theoretically studied and successfully applied in catalysis, molecular recognition, crystal engineering, etc. [19–26]. In addition, the role/behavior of the attached halogen atom in organic compounds can be classified into the following types: (i) as an electron with-

drawing substituent, (ii) as a halogen bond donor center, and (iii) as a noncovalent bond acceptor site.

On the other hand, the isoindole synthon is an important structural unit in many natural products and bioactive compounds, as well as a useful building-block for the construction of new *N*-containing heterocyclic compounds [27–34]. For instance, heterocyclic compounds containing isoindole moieties have demonstrated a promising biological action and pharmacological activity as pathogen antagonists [29]. The isoindole motif can also be involved as a versatile and powerful intermediate for the synthesis of various chiral heterocyclic compounds with unique properties [27–34]. Thus, the functionalization of isoindole moieties with noncovalent bond donor/acceptor sites can improve their photophysical properties [27], bioactivity [32], coordination ability [35,36], etc.

In this communication, our goal is to study the role of both electron withdrawing character and halogen bond donor ability of halogen atoms on Br · · · Ha (Ha = F, Cl, Br, I) interactions in a series of crystals of 4,5-dibromo-2-(4-substituted phenyl)hexahydro-3a,6-epoxyisoindol-1(4H)-ones (**3a–e**) (Scheme 1).



Scheme 1. Synthesis of **3a–e**.

2. Experimental Section

2.1. Materials and Instrumentation

All the chemicals were obtained from commercial sources (Acros Organics, Alfa Aesar) and used as received. Elemental analyses (C, H, N) were performed using a Eurovector EA 3000 (CHNS) elemental analyzer and were within $\pm 0.4\%$ of theoretical values. The infrared spectra ($4000\text{--}400\text{ cm}^{-1}$) were recorded on an IR-Fourier spectrometer Infracam FT-801 in KBr pellets. The ^1H and ^{13}C NMR spectra were recorded at room temperature on a Jeol JNM-ECA spectrometer operating at 600.2 and 150.9 MHz for ^1H and ^{13}C , respectively. The chemical shifts are reported in ppm using residual solvent peaks of chloroform as the internal references. Liquid chromatography mass spectra were taken on Thermo DSQ II-Focus GC (EI ionization, 200 °C source temperature, 70 eV, RTX-5MS column, helium carrier gas). Electrospray mass spectra (ESI-MS) were taken on Shimadzu LCMS-8040, equipped with dual ion source (DUIS) in electrospray positive mode (interface voltage 4.5 kV, nebulizer gas flow 2 L/min, drying gas flow 15 L/min, desolvation line temperature 250 °C, heating block temperature 400 °C).

2.2. Synthesis

2.2.1. Synthesis of 3a,6-epoxy-2,3,7,7a-tetrahydroisoindol-1-ones (2d,e)

General method: A solution of Et₃N (16.7 mL, 0.12 mol), acryloyl chloride (7.3 mL, 0.09 mol), and the corresponding amine 1 (0.06 mol) in toluene (100 mL) was heated under reflux for 7 h (TLC control, EtOAc–hexane, 1:1, Sorbfil). The mixture was cooled and poured into H₂O (100 mL). The resulting mixture was extracted with AcOEt (3 × 50 mL). The organic fractions were combined and dried over anhydrous Na₂SO₄. Solvent was evaporated under reduced pressure, and the residue was recrystallized from a hexane–AcOEt (for 2d) or EtOH–AcOEt mixture (for 2e).

(3a*RS*,6*RS*,7a*SR*)-2-(4-Bromophenyl)-2,3,7,7a-tetrahydro-3a,6-epoxyisoindol-1(6*H*)-one(2d). Yield 42%, m.p. 174–175 °C, beige thin plates. ^1H NMR (600.2 MHz, CDCl_3) δ 7.54 (d, $J \sim 9.1$ Hz, 2H, H-3, H-5 $\text{H}_{\text{arom.}}$), 7.46 (d, $J \sim 9.1$ Hz, 2H, H-4, H-6 $\text{H}_{\text{arom.}}$), 6.47–6.44 (m, 2H, H-4, H-5), 5.10 (d, $J \sim 4.5$ Hz, 1H, H-6), 4.43 (d, $J \sim 11.3$ Hz, 1H), 4.10 (d, $J \sim 11.3$ Hz, 1H, H-3), 2.63 (dd, $J \sim 3.5$ Hz, $J \sim 8.6$ Hz, 1H, H-7a), 2.29 (dt, $J \sim 3.5$ Hz, $J \sim 12.1$ Hz, 1H, H-7A), 1.67 (dd, $J \sim 8.6$ Hz, $J \sim 12.1$ Hz, 1H, H-7B) (see Figure S1). ^{13}C NMR (150.9 MHz, CDCl_3) δ 173.4, 138.4, 137.5 (2*C*_{arom.}), 132.8, 131.8, 121.4 (2*C*_{arom.}), 117.3, 87.8, 79.2, 50.6, 48.7, 28.9 (see Figure S1). IR (KBr): 1693 (NC=O). MS (EI, 70 eV): m/z = 307 [M $^+$] (82) (Br^{81}), 305 [M $^+$] (83) (Br^{79}), 276 (8), 250 (10), 171 (15), 155 (9), 134 (14), 81 (100), 55 (61), 53 (60). Anal. Calcd for $\text{C}_{14}\text{H}_{12}\text{BrNO}_2$: C, 54.95; H, 3.95; N, 4.58. Found: C, 54.91; H, 3.90; N, 4.69.

(3a*RS*,6*RS*,7a*SR*)-2-(4-Iodophenyl)-2,3,7,7a-tetrahydro-3a,6-epoxyisoindol-1(6*H*)-one(2e). Yield 51%, m.p. 185–186 °C, light beige fine needles. ^1H NMR (600.2 MHz, CDCl_3) δ 7.67 (d, $J \sim 8.9$ Hz, 2H, H-3, H-5 $\text{H}_{\text{arom.}}$), 7.44 (d, $J \sim 8.9$ Hz, 2H, H-4, H-6 $\text{H}_{\text{arom.}}$), 6.48–6.46 (m, 2H, H-4, H-5), 5.12 (dd, $J \sim 4.5$ Hz, $J \sim 1.5$ Hz, 1H, H-6), 4.43 (d, $J \sim 11.1$ Hz, 1H), 4.11 (d, $J \sim 11.1$ Hz, 1H, H-3), 2.63 (dd, $J \sim 3.5$ Hz, $J \sim 8.8$ Hz, 1H, H-7a), 2.29 (dt, $J \sim 3.5$ Hz, $J \sim 11.6$ Hz, 1H, H-7A), 1.67 (dd, $J \sim 8.8$ Hz, $J \sim 11.6$ Hz, 1H, H-7B) (see Figure S2). ^{13}C NMR (150.9 MHz, CDCl_3) δ 173.5, 139.1, 137.8 (2*C*_{arom.}), 137.5, 132.8, 121.7 (2*C*_{arom.}), 88.2, 87.8, 79.2, 50.6, 48.7, 28.9 (see Figure S2). IR (KBr): 1680 (NC=O). MS (EI, 70 eV): m/z = 353 [M $^+$] (100), 324 (10), 202 (4), 81 (46), 63 (7), 55 (42), 53 (35), 51 (8). Anal. Calcd for $\text{C}_{14}\text{H}_{12}\text{INO}_2$: C, 47.61; H, 3.43; N, 3.97. Found: C, 47.56; H, 3.37; N, 4.09.

2.2.2. Synthesis of 3a–e

Synthesis of 4,5-dibromohexahydro-3a,6-epoxyisoindol-1(4*H*)-ones 3a–f (general method): The solution of the corresponding isoindolone 2a–f (1.2 mmol) and the brominating agent (1.32 mmol) in 3 mL of dry chloroform was heated under reflux for 3–5 h (TLC control, EtOAc–hexane, 1:1). The reaction mixture was poured into H_2O (50 mL), extracted with CHCl_3 (3 × 20 mL), and combined organic parts were dried over anhydrous Na_2SO_4 ; the solvent was evaporated under reduced pressure, and the residue was recrystallized from a hexane–AcOEt mixture.

(3a*RS*,4*SR*,5*SR*,6*RS*,7a*SR*)-4,5-Dibromo-2-phenylhexahydro-3a,6-epoxyisoindol-1(4*H*)-one (3a). Yield 35%, m.p. 186–187 °C (decomp.), colorless prisms. ^1H NMR (600.2 MHz, CDCl_3) δ 7.62 (d, $J \sim 7.5$ Hz, 2H, H-2, H-6 $\text{H}_{\text{arom.}}$), 7.39 (t, $J \sim 7.5$ Hz, 2H, H-3, H-5 Ph $\text{H}_{\text{arom.}}$), 7.19 (t, $J \sim 7.5$ Hz, 1H, H-4 $\text{H}_{\text{arom.}}$), 4.75 (t, $J \sim 5.1$ Hz, 1H, H-6), 4.51 (ddd, $J \sim 1.4$ Hz, $J \sim 2.7$ Hz, $J \sim 5.1$ Hz, 1H, H-5), 4.25 (d, $J \sim 2.7$ Hz, 1H, H-4), 4.10 (d, $J \sim 11.7$ Hz, 1H), 4.04 (d, $J \sim 11.7$ Hz, 1H, H-3), 2.94 (dd, $J \sim 4.8$ Hz, $J \sim 9.6$ Hz, 1H, H-7a), 2.79 (dd, $J \sim 9.6$ Hz, $J \sim 13.4$ Hz, 1H, H-7B), 2.31 (ddt, $J \sim 1.4$ Hz, $J \sim 13.4$ Hz, $J \sim 4.8$ Hz, 1H, H-7A) (see Figure S3). ^{13}C NMR (150.9 MHz, CDCl_3) δ 172.2, 138.6, 129.0, 125.2 (2*C*_{arom.}), 120.1 (2*C*_{arom.}), 89.0, 80.9, 55.8, 54.0, 50.7, 49.5, 30.8 (see Figure S3). IR (KBr): 1671 (NC=O). MS (EI, 70 eV): m/z = 389 [M $^+$] (Br^{81}) (51), 387 [M $^+$] (84) (Br^{81} , Br^{79}), 385 [M $^+$] (Br^{79}) (51), 385 (46), 308 (62), 227 (24), 209 (11), 198 (18), 183 (18), 144 (14), 119 (14), 106 (38), 104 (58), 91 (14), 81 (50), 77 (100), 65 (34), 55 (51), 51 (40). Anal. Calcd for $\text{C}_{14}\text{H}_{13}\text{Br}_2\text{NO}_2$: C, 43.44; H, 3.39; N, 3.62. Found: C, 43.40; H, 3.33; N, 3.74.

(3a*RS*,4*SR*,5*SR*,6*RS*,7a*SR*)-4,5-Dibromo-2-(4-fluorophenyl)hexahydro-3a,6-epoxyisoindol-1(4*H*)-one (3b). Yield 20 %, m.p. > 195 °C (decomp.), colorless fine needles. ^1H NMR (600.2 MHz, CDCl_3) δ 7.59–7.57 (m, 2H, H-3, H-5 $\text{H}_{\text{arom.}}$), 7.10–7.07 (m, 2H, H-2, H-6 $\text{H}_{\text{arom.}}$), 4.76 (t, $J \sim 5.0$ Hz, 1H, H-6), 4.51 (ddd, $J \sim 5.0$ Hz, $J \sim 1.0$ Hz, $J \sim 2.5$ Hz, 1H, H-5), 4.25 (d, $J \sim 2.5$ Hz, 1H, H-4), 4.09 (d, $J \sim 11.6$ Hz, 1H), 4.01 (d, $J \sim 11.6$ Hz, 1H, H-3), 2.95 (dd, $J \sim 4.5$ Hz, $J \sim 9.6$ Hz, 1H, H-7a), 2.80 (dd, $J \sim 9.6$ Hz, $J \sim 13.1$ Hz, 1H, H-7B), 2.30 (ddt, $J \sim 13.1$ Hz, $J \sim 1.0$ Hz, $J \sim 4.5$ Hz, 1H, H-7A) (see Figure S4). ^{13}C NMR (150.9 MHz, CDCl_3) δ 172.1, 159.8 (d, $J \sim 245.6$ Hz), 134.7 (d, $J \sim 2.9$ Hz), 122.1 (d, $J \sim 7.2$ Hz, 2C), 115.7 (d, $J \sim 20.2$ Hz, 2C), 88.9, 80.9, 55.6, 53.9, 51.0, 49.4, 30.8 (see Figure S4). ^{19}F NMR (564.7 MHz, CDCl_3) δ –116.3. IR (KBr): 1703 (NC=O). MS (ESI): m/z = 406 [M + H $^+$]. Anal. Calcd for $\text{C}_{14}\text{H}_{12}\text{Br}_2\text{FNO}_2$: C, 41.51; H, 2.99; N, 3.46. Found: C, 41.47; H, 2.94; N, 3.55.

(3aRS,4SR,5SR,6RS,7aSR)-4,5-Dibromo-2-(4-chlorophenyl)hexahydro-3a,6-epoxyisoindol-1(4H)-one (3c). Yield 25%, m.p. 191–192 °C, colorless plates. ^1H NMR (600.2 MHz, CDCl_3) δ 7.58 (d, $J \sim 9.1$ Hz, 2H, H-3, H-5 $\text{H}_{\text{arom.}}$), 7.35 (d, $J \sim 9.1$ Hz, 2H, H-2, H-6 $\text{H}_{\text{arom.}}$), 4.76 (t, $J \sim 5.0$ Hz, 1H, H-6), 4.51 (ddd, $J \sim 5.0$ Hz, $J \sim 1.0$ Hz, $J \sim 2.5$ Hz, 1H, H-5), 4.24 (d, $J \sim 2.5$ Hz, 1H, H-4), 4.07 (d, $J \sim 11.6$ Hz, 1H), 4.01 (d, $J \sim 11.6$ Hz, 1H, H-3), 2.94 (dd, $J \sim 4.5$ Hz, $J \sim 9.6$ Hz, 1H, H-7a), 2.80 (dd, $J \sim 9.6$ Hz, $J \sim 13.1$ Hz, 1H, H-7B), 2.30 (ddt, $J \sim 13.1$ Hz, $J \sim 1.0$ Hz, $J \sim 4.5$ Hz, 1H, H-7A) (see Figure S5). ^{13}C NMR (150.9 MHz, CDCl_3) δ 172.2, 137.2, 130.2, 129.0 (2C), 121.1 (2C), 88.8, 80.9, 55.6, 53.8, 50.6, 49.5, 30.8 (see Figure S5). IR (KBr): 1694 (NC=O). MS (ESI): $m/z = 422$ [M + H^+] (Cl^{35}), 424 [M + H^+] (Cl^{37}). Anal. Calcd for $\text{C}_{14}\text{H}_{12}\text{Br}_2\text{ClNO}_2$: C, 39.89; H, 2.87; N, 3.32. Found: C, 39.84; H, 2.83; N, 3.43.

(3aRS,4SR,5SR,6RS,7aSR)-4,5-Dibromo-2-(4-bromophenyl)hexahydro-3a,6-epoxyisoindol-1(4H)-one (3d). Yield 24%, m.p. > 185 °C (decomp.), colorless fine needles. ^1H NMR (600.2 MHz, CDCl_3) δ 7.54 (d, $J \sim 9.1$ Hz, 2H, H-3, H-5 $\text{H}_{\text{arom.}}$), 7.49 (d, $J \sim 9.1$ Hz, 2H, H-2, H-6 $\text{H}_{\text{arom.}}$), 4.76 (t, $J \sim 4.7$ Hz, 1H, H-6), 4.51 (ddd, $J \sim 4.7$ Hz, $J \sim 1.3$ Hz, $J \sim 2.5$ Hz, 1H, H-5), 4.25 (d, $J \sim 2.5$ Hz, 1H, H-4), 4.07 (dd, $J \sim 1.5$ Hz, $J \sim 11.6$ Hz, 1H), 4.01 (dd, $J \sim 1.5$ Hz, $J \sim 11.6$ Hz, 1H, H-3), 2.94 (dd, $J \sim 4.7$ Hz, $J \sim 9.5$ Hz, 1H, H-7a), 2.80 (ddd, $J \sim 1.5$ Hz, $J \sim 9.5$ Hz, $J \sim 13.1$ Hz, 1H, H-7B), 2.30 (ddt, $J \sim 13.1$ Hz, $J \sim 1.3$ Hz, $J \sim 4.7$ Hz, 1H, H-7A) (see Figure S6). ^{13}C NMR (150.9 MHz, CDCl_3) δ 172.3, 137.7, 132.0 (2C), 121.4 (2C), 118.0, 88.8, 80.9, 55.6, 53.8, 50.6, 49.6, 30.9 (see Figure S6). IR (KBr): 1694 (NC=O). MS (ESI): $m/z = 467$ [M + H^+]. Anal. Calcd for $\text{C}_{14}\text{H}_{12}\text{Br}_3\text{NO}_2$: C, 36.09; H, 2.60; N, 3.01. Found: C, 36.05; H, 2.56; N, 3.14.

(3aRS,4SR,5SR,6RS,7aSR)-4,5-Dibromo-2-(4-iodophenyl)hexahydro-3a,6-epoxyisoindol-1(4H)-one (3e). Yield 18%, m.p. > 205 °C (decomp.), light beige plates. ^1H NMR (600.2 MHz, CDCl_3) δ 7.68 (dt, $J \sim 9.1$ Hz, $J \sim 2.5$ Hz, 2H, H-3, H-5 $\text{H}_{\text{arom.}}$), 7.41 (dt, $J \sim 9.1$ Hz, $J \sim 2.5$ Hz, 2H, H-2, H-6 $\text{H}_{\text{arom.}}$), 4.75 (t, $J \sim 5.0$ Hz, 1H, H-6), 4.51 (ddd, $J \sim 5.0$ Hz, $J \sim 1.2$ Hz, $J \sim 2.5$ Hz, 1H, H-5), 4.24 (d, $J \sim 2.5$ Hz, 1H, H-4), 4.06 (d, $J \sim 12.1$ Hz, 1H), 4.01 (d, $J \sim 12.1$ Hz, 1H, H-3), 2.93 (dd, $J \sim 4.5$ Hz, $J \sim 9.1$ Hz, 1H, H-7a), 2.79 (dd, $J \sim 9.1$ Hz, $J \sim 13.1$ Hz, 1H, H-7B), 2.29 (ddt, $J \sim 13.1$ Hz, $J \sim 1.2$ Hz, $J \sim 4.5$ Hz, 1H, H-7A) (see Figure S7). ^{13}C NMR (150.9 MHz, CDCl_3) δ 172.3, 138.4, 137.9 (2C), 121.6 (2C), 88.8, 88.7, 80.9, 55.5, 53.8, 50.4, 49.6, 30.8 (see Figure S7). IR (KBr): 1697 (NC=O). MS (ESI): $m/z = 514$ [M + H^+]. Anal. Calcd for $\text{C}_{14}\text{H}_{12}\text{Br}_2\text{INO}_2$: C, 32.79; H, 2.36; N, 2.73. Found: C, 32.76; H, 2.32; N, 2.82.

2.3. X-ray Analysis

X-ray diffraction analyses were performed at the Center for Shared Use of Physical Methods of Investigation at the Frumkin Institute of Physical Chemistry and Electrochemistry, RAS (CKP FMI IPCE RAS). Single crystals of compounds 3a–e (Table 1) for X-ray crystallography were grown by slow recrystallization of samples from EtOAc/hexane mixtures. Suitable single crystals were selected, immersed in an inert oil, mounted on a glass fiber, and attached to a goniometer head.

The X-ray diffraction data were collected on a Bruker Kappa Apex II automatic four-circle diffractometer equipped with an area detector (Mo-K α sealed-tube X-ray source, $\lambda = 0.71073$ Å, graphite monochromator) at 296 K for all compounds except 3a, measured at 100 K.

The data frames were collected using the program APEX2 and processed using the program SAINT routine within APEX2. The unit cell parameters were refined over the whole dataset [37]. The data were corrected for absorption on the multi-scan technique as implemented in SADABS [38]. The structures were solved by direct method using SHELXS and refined by full-matrix least-squares on F^2 using SHELXL-2018 software [39] in the anisotropic approximation for all non-hydrogen atoms. Hydrogen atoms on carbon were calculated in ideal positions with isotropic displacement parameters set to $1.2 \times U_{\text{eq}}(\text{C})$.

Atomic coordinates for compounds 3a–e have been deposited with the Cambridge Crystallographic Data Centre. CCDC numbers are 2036862, 2036839, 2036841, 2036840, and 2036843. The supplementary crystallographic data can be obtained free of charge from the Cambridge Crystallographic Data Centre via www.ccdc.cam.ac.uk/data_request/cif.

Copies of this information may be obtained free of charge from the Director, CCDC, Cambridge, UK (www.ccdc.cam.ac.uk).

Table 1. Crystallographic data and structure refinement details for 3a–e.

| | 3a | 3b | 3c | 3d | 3e |
|--|---|--|---|---|--|
| Empirical Formula | C ₁₄ H ₁₃ Br ₂ NO ₂ | C ₁₄ H ₁₂ Br ₂ FNO ₂ | C ₁₄ H ₁₂ Br ₂ ClNO ₂ | C ₁₄ H ₁₂ Br ₃ NO ₂ | C ₁₄ H ₁₂ Br ₂ INO ₂ |
| <i>fw</i> | 387.07 | 405.07 | 421.52 | 465.98 | 512.97 |
| Temperature (K) | 100(2) | 296(2) | 296(2) | 296(2) | 296(2) |
| Crystal System | Triclinic | Orthorhombic | Monoclinic | Monoclinic | Monoclinic |
| Space Group | P-1 | Pca2 ₁ | C2/c | P2 ₁ /c | P2 ₁ /c |
| a (Å) | 7.490(2) | 22.4191(5) | 19.3156(6) | 6.7008(3) | 6.6621(3) |
| b (Å) | 8.896(3) | 8.2335(2) | 6.7072(2) | 18.3496(8) | 18.4894(8) |
| c (Å) | 11.997(3) | 7.5976(2) | 24.5261(8) | 24.9667(13) | 25.6634(11) |
| α | 108.201(4) | 90 | 90 | 90 | 90 |
| β | 91.053(4) | 90 | 110.555(2) | 95.417(3) | 97.487(2) |
| γ | 112.877(4) | 90 | 90 | 90 | 90 |
| V (Å ³) | 690.6(3) | 1402.42(6) | 2975.15(16) | 3056.1(2) | 3134.2(2) |
| Z | 2 | 4 | 8 | 8 | 8 |
| ρ_{calc} (g cm ⁻³) | 1.861 | 1.918 | 1.882 | 2.025 | 2.174 |
| μ (Mo K α) (mm ⁻¹) | 5.865 | 5.791 | 5.628 | 7.919 | 7.143 |
| F(000) | 380 | 792 | 1648 | 1792 | 1936 |
| GOOF | 1.021 | 1.029 | 1.013 | 1.031 | 1.001 |
| R1 ^a (I $\geq 2\sigma$) | 0.0294 | 0.0307 | 0.0369 | 0.0572 | 0.0495 |
| wR2 ^b (I $\geq 2\sigma$) | 0.0755 | 0.0591 | 0.0657 | 0.1152 | 0.0883 |

$$^a R1 = \sum |F_o| - |F_c| | / \sum |F_o| . \quad ^b wR2 = \{\sum [w(F_o^2 - F_c^2)^2] / \sum [w(F_o^2)^2]\}^{1/2} .$$

3. Results

The 2-(4-substituted phenyl)-2,3,7,7a-tetrahydro-3a,6-epoxyisoindol-1(6H)-ones (2a–e) were synthesized by the known reaction of acryloyl chloride with the corresponding 4-substituted-N-(furan-2-ylmethyl)anilines (1a–e) in the presence of Et₃N in toluene (Scheme 1) [31,33,40–43]. Compounds 2d and 2e are novel, whereas 2a–c have been reported earlier [31,33,40–43], and hence will not be discussed herein. The structures of 2d and 2e were deduced from their IR, ¹H and ¹³C NMR spectra (Figures S1 and S2), ESI-MS, and elemental analysis (see experimental section). The IR spectra of 2d and 2e reveal the presence of ν(C=O) vibrations at ca. 1693 and 1680 cm⁻¹, respectively. The ¹H and ¹³C NMR spectra in CDCl₃ show the characteristic signals of C_{7a}–H and C=O groups at 2.63 and 173.4 ppm for 2d and 2.63 and 173.5 ppm for 2e. Both ESI-MS and elemental analysis are consistent with the proposed formulations.

Next, the reaction of 2-(4-substituted phenyl)-2,3,7,7a-tetrahydro-3a,6-epoxyisoindol-1(6H)-ones (2a–e) with [(Me₂NCO)₂H]Br₃ in dry chloroform under reflux leads to the corresponding 4,5-dibromo-2-(4-substituted phenyl)hexahydro-3a,6-epoxy-isoindol-1(4H)-ones (3a–e) in yields of 18–35% (Scheme 1).

The ¹H NMR spectra of 3a–e in CDCl₃ solution at room temperature show a resonance at δ 2.92–2.99, which can be assigned to the proton of the C_{7a}–H group (Figures S3–S7). In the ¹³C NMR spectra of 3a–e, the carbon atom of C=O was found at 172.1–172.7 ppm (Figures S3–S7). Not only electron-withdrawing properties of para-substituents, but also their noncovalent bond donor or acceptor character leads to the chemical shift of C_{Ar}–Ha in the ¹³C NMR spectra of 3a–e: 129.0 (H), 160.6 (F), 130.2 (Cl), 118.0 (Br), and 88.8 (I) ppm. Contribution of halogen bonding on chemical shift of C_{Ar}–Ha in the ¹³C NMR spectra of 3a–e is not clear, because there is no intermolecular halogen bonding in compounds 3b and 3c (see below). Moreover, ESI-MS and elemental analyses also confirm the chemical structures of 3a–e.

The crystal structures of 3a–e were determined by single crystal X-ray diffraction and are shown in Figure 1 along with the atomic numbering schemes. In contrast to 3a–c, both compounds 3d and 3e crystallize with two molecules in the asymmetric unit, of which only one is illustrated in Figure 1. An important feature of the compounds is the presence of the 3aS,4R,5R,6S,7aR and 3aR,4S,5S,6R,7aS stereogenic carbon centers in 3a–c and 3d,e, respectively (Figure 1). The different configurations seem to be driven by intermolecular interactions in the bromination of 2a–c into 3a–c. The para-halogen substituents have a remarkable effect on the $\angle \text{C1}–\text{N2}–\text{C11}–\text{C16}$ (for 3a–c) dihedral angles ($^{\circ}$): 25.7 (–H), –46.2 (–F), 15.9 (–Cl), –19.1 (–Br), and –19.3 (–I), i.e., aryl and pyrrolidone rings are not co-planar (Figure 1). Moreover, there is no trend between the dihedral angles and the electron-withdrawing character of the substituents.

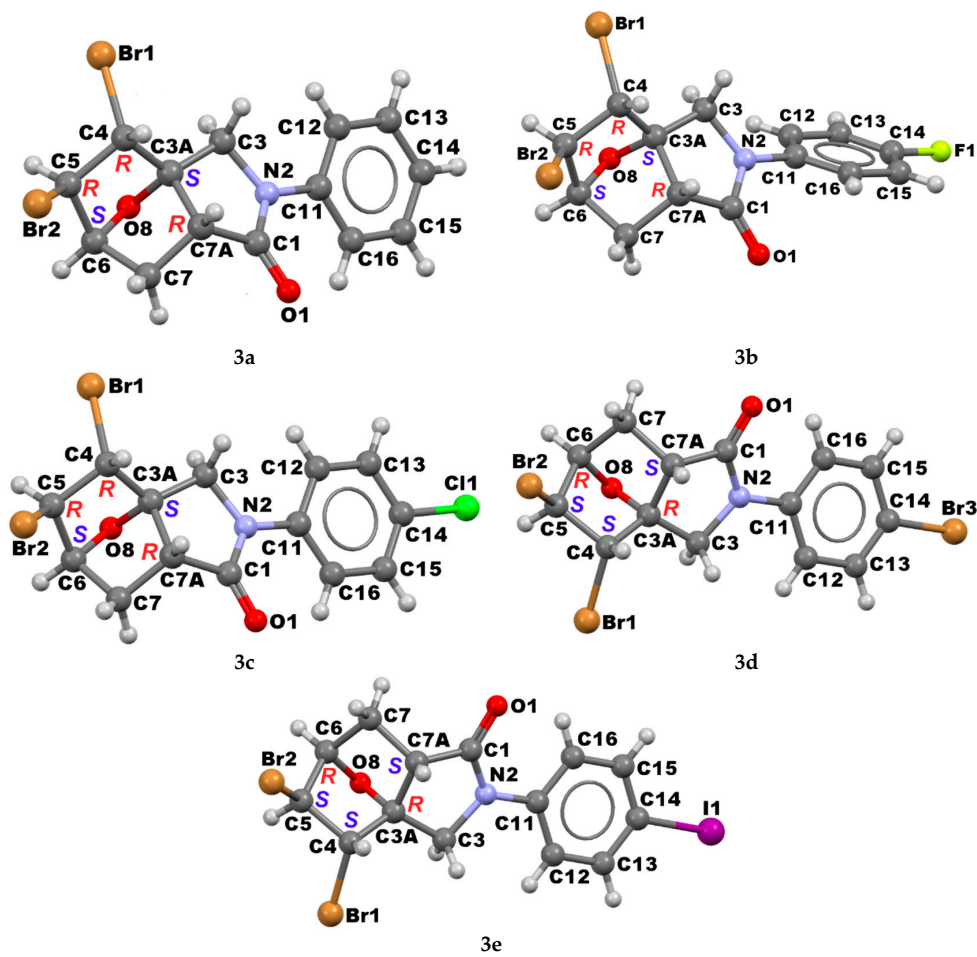


Figure 1. X-ray structure of 3a–e.

Although all 3a–e have at least two potential halogen bond donor centers (Br atoms in the isoindole moiety), there is no intermolecular halogen bonding in the compounds 3b and 3c. In the packing of 3a–e, the most noticeable intermolecular features are C–H \cdots O, C–H \cdots Br, and C–H \cdots π hydrogen bonds, which can also cooperate with C–Br \cdots Br, C–Br \cdots π , and C–I \cdots I types of halogen bonds.

In the crystal of 3a, the molecules are interacting through Br \cdots Br type II [3,44–46] of halogen bonding to form a 1D supramolecular chain along the *b*-axis [47], depicted in Figure 2. The Br(1) \cdots Br(2) distance (3.638 Å) is shorter than twice the sum of the Bondi's van der Waals radii of the interacting atoms (Br + Br = 1.85 + 1.85 = 3.70 Å) [48], and the $\angle \text{C}(4)–\text{Br}(1)\cdots\text{Br}(2)$ angle is 169.68°.

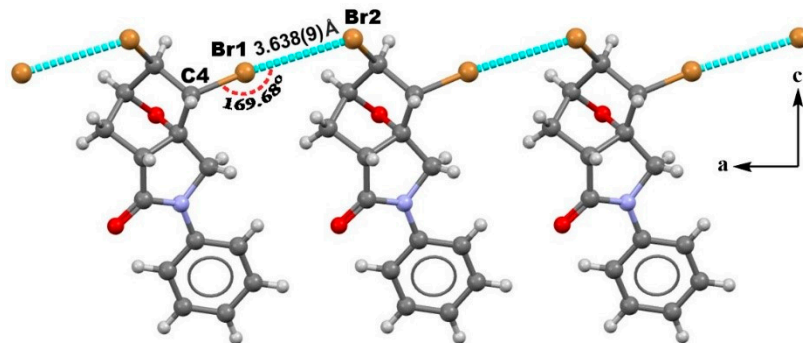


Figure 2. Partial view of the 1D chain formed through $\text{C}-\text{Br}\cdots\text{Br}$ halogen bonds in the crystal structure of 3a.

Compounds 3d and 3e have two molecules in the unit cell, and both molecules are similarly involved in intermolecular interactions. Both $\text{C}_{\text{Ar}}-\text{Br}\cdots\text{Br}$ (angle of 164.51°) and $\text{C}_{\text{Ar}}-\text{I}\cdots\text{I}$ (angle of 163.08°) type I halogen bonding distances of 3.486 and 3.679 Å, respectively, are significantly shorter than the sum of the Bondi's van der Waals radii of the interacting atoms ($\text{Br} + \text{Br} = 1.85 + 1.85 = 3.70$ Å and $\text{I} + \text{I} = 1.98 + 1.98 = 3.96$ Å [48]) (Figure 3). Intermolecular $\text{Br}\cdots\pi$ and $\text{I}\cdots\pi$ interactions also contribute to the formation of 2D sheets in 3d and 3e, respectively, in which the bond parameters such as $\text{Ha}\cdots\pi$ distances and $\angle \text{C}-\text{Ha}\cdots\pi$ angles are dependent on the nature of halogen atom (Figure 3). In contrast to 3e, there is a weak type II halogen bonding $\text{C}(5)-\text{Br}(2)\cdots\text{Br}(22)$ (angle of 158.46°) with distance of 3.644 Å in 3d, which links the molecules into a 1D chain (Figure 3a).

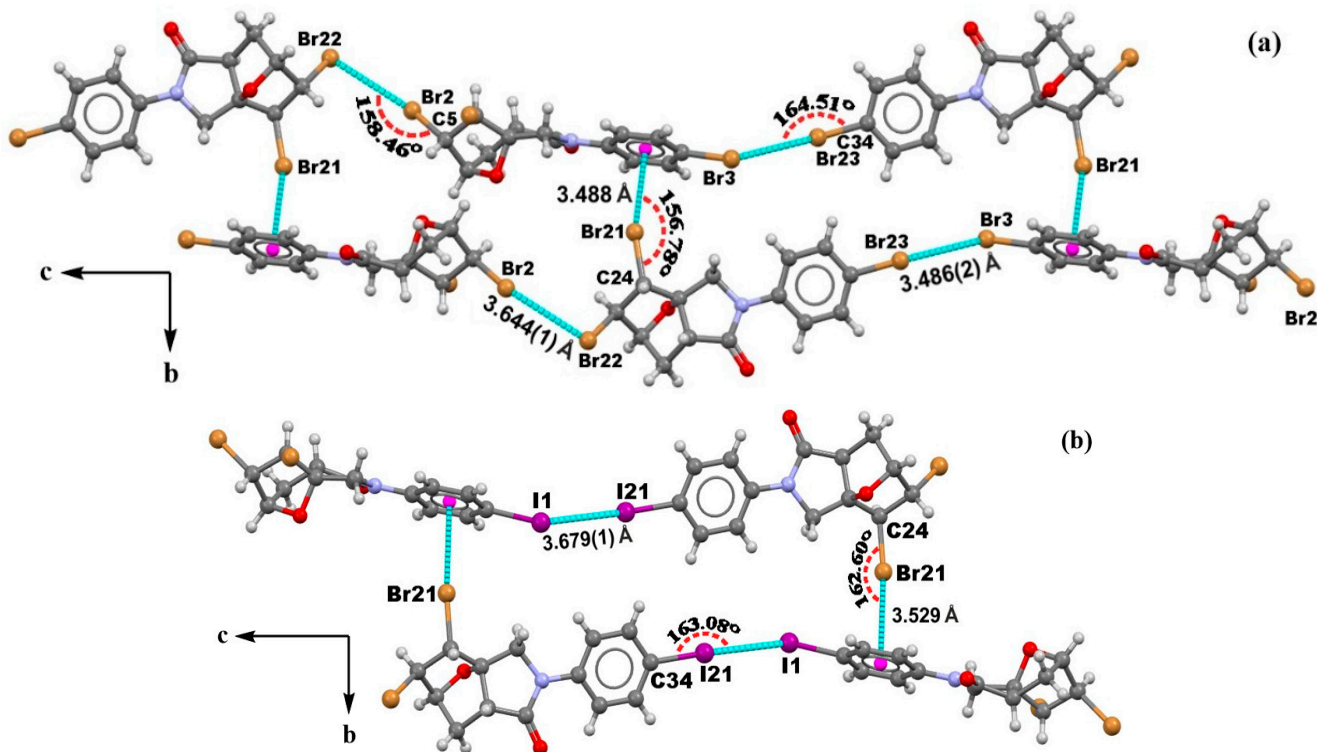


Figure 3. Intermolecular $\text{Ha}\cdots\text{Ha}$ and $\text{Ha}\cdots\pi$ types of halogen bonding in 3d (a) and 3e (b).

Cooperation of $\text{C}-\text{H}\cdots\text{O}$, $\text{C}-\text{H}\cdots\text{Br}$, and $\text{C}-\text{H}\cdots\pi$ hydrogen bonds with the $\text{Br}\cdots\text{Br}$ halogen bonding in the crystal packing of 3a leads to 2D sheets (Figure S8). In contrast to 3a, the bromine atom behaves only as the hydrogen bond acceptor in 3b and 3c affording 3D supramolecular architectures (Figures S9 and S10). In 3c, the attached

para-Cl also engages in weak intermolecular hydrogen bonding to support the molecules to orient in a head-to-tail arrangement in 3D networks (Figure S10). Not only intermolecular hydrogen bonds, but both $\text{Br}\cdots\pi$ and $\text{Ha}\cdots\text{Ha}$ types of halogen bond in 3d and 3e play an important role in directing the crystal packing and in the formation of 3D structures (Figures S11 and S12).

4. Conclusions

Both physical and chemical properties of functional materials in the solid state can be controlled by noncovalent interactions between molecular building blocks. A suitable design of molecular units with noncovalent bond donor or acceptor sites is an important strategy to control and improve the properties and the function of materials. The noncovalent bond donor ability of halogen atoms allows to generate new supramolecular networks via halogen bonding, which is dependent on the nature of the halogen atom.

Herein, the role of para-halogen substituents in intermolecular halogen bonding in a series of 4,5-dibromo-2-(4-substituted phenyl)hexahydro-3a,6-epoxyisoindol-1(4H)-ones was analyzed. Both substituents 4-F (3b) and 4-Cl (3c) are not involved in intermolecular halogen bond formation, whereas $\text{Br}\cdots\text{Br}$ (in 4-H), $\text{Br}\cdots\text{Br}$ and $\text{Br}\cdots\pi$ (in 4-Br), and $\text{I}\cdots\text{I}$ and $\text{Br}\cdots\pi$ (in 4-I) types of interactions are observed in 3a, 3d, and 3e, respectively. The $\text{Ha}\cdots\text{Ha}$ and $\text{Ha}\cdots\pi$ halogen bonds cooperate with other types of noncovalent interactions in the crystal packing of the studied molecules leading to 2D sheets or 3D supramolecular architectures.

Supplementary Materials: The following are available online at <https://www.mdpi.com/2073-4352/11/2/112/s1>, $^1\text{H}/^{13}\text{C}$ NMR spectra of 2d,e and 3a–e (Figures S1–S7), packing diagrams of 3a–e (Figures S8–S12).

Author Contributions: Conceptualization, F.I.Z. and A.V.G.; methodology, H.H.T.; investigation, D.F.M., M.A.N. and E.V.N.; resources, M.S.G.; data curation, V.P.Z.; writing—original draft preparation, F.I.Z., A.V.G. and K.T.M.; writing—review and editing, V.P.Z. and M.S.G.; visualization, H.H.T.; supervision, A.J.L.P. All authors have read and agreed to the published version of the manuscript.

Institutional Review Board Statement: Not applicable.

Informed Consent Statement: Not applicable.

Data Availability Statement: Not applicable.

Acknowledgments: Funding for this research was provided by the Ministry of Education and Science of the Russian Federation (award No. 075-03-2020-223 (FSSF-2020-0017)). This work was also supported by the Fundação para a Ciéncia e Tecnologia (FCT), project UIDB/00100/2020 of Centro de Química Estrutural. This paper has been supported by the RUDN University Strategic Academic Leadership Program (A.J.L.P.). K.T.M and A.V.G acknowledge the FCT and Instituto Superior Técnico DL 57/2016 and L 57/2017 Program, Contracts no: IST-ID/85/2018 and IST-ID/110/2018, respectively. The authors also acknowledge the financial support by the Baku State University, Azerbaijan.

Conflicts of Interest: The authors declare no conflict of interest.

References

- Metrangolo, P.; Resnati, G. (Eds.) *Halogen Bonding: Fundamentals and Applications (Structure and Bonding)*; Springer: Heidelberg, Germany, 2010.
- Priimagi, A.; Cavallo, G.; Metrangolo, P.; Resnati, G. The Halogen Bond in the Design of Functional Supramolecular Materials: Recent Advances. *Acc. Chem. Res.* **2013**, *48*, 2686–2695. [[CrossRef](#)] [[PubMed](#)]
- Desiraju, G.R.; Ho, P.S.; Kloo, L.; Legon, A.C.; Marquardt, R.; Metrangolo, P.; Politzer, P.; Resnati, G.; Rissanen, K. Definition of the halogen bond (IUPAC Recommendations 2013). *Pure Appl. Chem.* **2013**, *85*, 1711–1713. [[CrossRef](#)]
- Cavallo, G.; Metrangolo, P.; Milani, R.; Pilati, T.; Priimagi, A.; Resnati, G.; Terraneo, G. The halogen bond. *Chem. Rev.* **2016**, *116*, 2478–2601. [[CrossRef](#)] [[PubMed](#)]
- Wang, C.-G.; Chong, A.M.L.; Pan, H.M.; Sarkar, J.; Tay, X.T.; Goto, A. Recent development in halogen-bonding catalyzed living radical polymerization. *Polym. Chem.* **2020**, *11*, 5559–5571. [[CrossRef](#)]
- Sutar, R.L.; Huber, S.M. Catalysis of Organic Reactions through Halogen Bonding. *ACS Catal.* **2019**, *9*, 9622–9639. [[CrossRef](#)]

7. Wilcken, R.; Zimmermann, M.O.; Lange, A.; Joerger, A.C.; Boeckler, F.M. Principles and Applications of Halogen Bonding in Medicinal Chemistry and Chemical Biology. *J. Med. Chem.* **2013**, *56*, 1363–1388. [[CrossRef](#)]
8. Maharramov, A.M.; Mahmudov, K.T.; Kopylovich, M.N.; Pombeiro, A.J.L. (Eds.) *Non-Covalent Interactions in the Synthesis and Design of New Compounds*; John Wiley & Sons: Hoboken, NJ, USA, 2016.
9. Mahmudov, K.T.; Kopylovich, M.N.; Pombeiro, A.J.L. (Eds.) *Noncovalent Interactions in Catalysis*; RSC Publishing: Cambridge, UK, 2019.
10. Mahmudov, K.T.; Kopylovich, M.N.; Guedes da Silva, M.F.C.; Pombeiro, A.J.L. Non-covalent interactions in the synthesis of coordination compounds: Recent advances. *Coord. Chem. Rev.* **2017**, *345*, 54–72. [[CrossRef](#)]
11. Mahmudov, K.T.; Gurbanov, A.V.; Guseinov, F.I.; Guedes da Silva, M.F.C. Noncovalent interactions in metal complex catalysis. *Coord. Chem. Rev.* **2019**, *387*, 32–46. [[CrossRef](#)]
12. Mahmudov, K.T.; Gurbanov, A.V.; Aliyeva, V.A.; Resnati, G.; Pombeiro, A.J.L. Pnictogen bonding in coordination chemistry. *Coord. Chem. Rev.* **2020**, *418*, 213381. [[CrossRef](#)]
13. Berger, G.; Frangville, P.; Meyer, F. Halogen bonding for molecular recognition: New developments in materials and biological sciences. *Chem. Commun.* **2020**, *56*, 4970–4981. [[CrossRef](#)]
14. Groom, C.R.; Bruno, I.J.; Lightfoot, M.P.; Ward, S.C. The Cambridge Structural Database. *Acta Cryst.* **2016**, *72*, 171–179. [[CrossRef](#)] [[PubMed](#)]
15. Ivanov, D.M.; Kinzhalov, M.A.; Novikov, A.S.; Ananyev, I.V.; Romanova, A.A.; Boyarskiy, V.P.; Haukka, M.; Kukushkin, V.Y. $\text{H}_2\text{C}(\text{X})-\text{X}\cdots\text{X}-(\text{X}=\text{Cl}, \text{Br})$ Halogen Bonding of Dihalomethanes. *Cryst. Growth Des.* **2017**, *17*, 1353–1362. [[CrossRef](#)]
16. Wu, J.T.; Li, J.X.; Miao, X.R.; Ying, L.; Dong, M.Q.; Deng, W.L. The $\text{Br}\cdots\pi$ halogen bond assisted self-assembly of an asymmetric molecule regulated by concentration. *Chem. Commun.* **2020**, *56*, 2727–2730. [[CrossRef](#)] [[PubMed](#)]
17. Forni, A. Experimental and Theoretical Study of the $\text{Br}\cdots\text{N}$ Halogen Bond in Complexes of 1,4-Dibromotetrafluorobenzene with Dipyridyl Derivatives. *J. Phys. Chem. A* **2009**, *113*, 3403–3412. [[CrossRef](#)]
18. Loy, C.; Zeller, M.; Rosokha, S.V. Halogen Bonding in the Complexes of Brominated Electrophiles with Chloride Anions: From a Weak Supramolecular Interaction to a Covalent $\text{Br}-\text{Cl}$ Bond. *Crystals* **2020**, *10*, 1075. [[CrossRef](#)]
19. Bauza, A.; Quinonero, D.; Frontera, A.; Deya, P.M. Substituent effects in halogen bonding complexes between aromatic donors and acceptors: A comprehensive ab initio study. *Phys. Chem. Chem. Phys.* **2011**, *13*, 20371–20379. [[CrossRef](#)]
20. Solimannejad, M.; Malekani, M.; Alkorta, I. Substituent effects on the cooperativity of halogen bonding. *J. Phys. Chem. A* **2013**, *117*, 5551–5557. [[CrossRef](#)]
21. Domagała, M.; Palusiak, M. The influence of substituent effect on noncovalent interactions in ternary complexes stabilized by hydrogen-bonding and halogen-bonding. *Comput. Theor. Chem.* **2014**, *1027*, 173–178. [[CrossRef](#)]
22. Sutradhar, D.; Chandra, A.K. Cl \cdots Cl Halogen Bonding: Nature and Effect of Substituent at Electron Donor Cl atom. *ChemistrySelect* **2020**, *5*, 554–563. [[CrossRef](#)]
23. Zhang, Q.; Smalley, A.; Zhu, Z.; Xu, Z.; Peng, C.; Chen, Z.; Yao, G.; Shi, J.; Zhu, W. Computational study of the substituent effect of halogenated fused-ring heteroaromatics on halogen bonding. *J. Mol. Mod.* **2020**, *26*, 270. [[CrossRef](#)]
24. Tao, Y.; Qiu, Y.; Zou, W.; Nanayakkara, S.; Yannacone, S.; Kraka, E. In Situ Assessment of Intrinsic Strength of X-I \cdots OA-Type Halogen Bonds in Molecular Crystals with Periodic Local Vibrational Mode Theory. *Molecules* **2020**, *25*, 1589. [[CrossRef](#)] [[PubMed](#)]
25. Alkorta, I.; Elguero, J.; Frontera, A. Not Only Hydrogen Bonds: Other Noncovalent Interactions. *Crystals* **2020**, *10*, 180. [[CrossRef](#)]
26. Dumitrescu, D.; Shova, S.; Man, I.C.; Caira, M.R.; Popa, M.M.; Dumitrescu, F. 5-Iodo-1-Arylpyrazoles as Potential Benchmarks for Investigating the Tuning of the Halogen Bonding. *Crystals* **2020**, *10*, 1149. [[CrossRef](#)]
27. Chamas, Z.; Marchi, E.; Presson, B.; Aubert, E.; Fort, Y.; Ceroni, P.; Mamane, V. Synthesis and Solid-state Fluorescence Properties of Pentacyclic 7-Substituted-indeno[1',2':4,5]pyrido[2,1-a]soindol-5-ones. *RSC Adv.* **2015**, *5*, 2715–2723. [[CrossRef](#)]
28. Zhou, Q.-F.; Ge, F.-F.; Chen, Q.-Q.; Lu, T. Construction of pyrazolo[5,1-a]isoindol-8(3aH)-one derivatives via phosphine-catalyzed cyclization of electron-deficient alkynes and N-amino substituted phthalimide. *RSC Adv.* **2016**, *6*, 1395–1402. [[CrossRef](#)]
29. Xie, J.-N.; Yu, B.; Guo, C.-X.; He, L.-N. Copper(I)/phosphine-catalyzed tandem carboxylation/annulation of terminal alkynes under ambient pressure of CO_2 : One-pot access to 3a-hydroxyisoxazolo[3,2-a]isoindol-8(3aH)-ones. *Green Chem.* **2015**, *17*, 4061–4067. [[CrossRef](#)]
30. Nadirova, M.A.; Pokazeev, K.M.; Kolesnik, I.A.; Dorovatovskii, P.V.; Bumagin, N.A.; Potkin, V.I. Synthesis and structure of esterification products of 6-aryl-1,2,3,6,7,7a-hexahydro-3a,6-epoxyisoindole-7-carboxylic acids. *Chem. Heterocycl. Compd.* **2019**, *55*, 729–738. [[CrossRef](#)]
31. Zubkov, F.I.; Zaytsev, V.P.; Nikitina, E.V.; Khrustalev, V.N.; Gozun, S.V.; Boltukhina, E.V.; Varlamov, A.V. Skeletal. Wagner-Meerwein rearrangement of perhydro-3a,6,4,5-diepoxyisoindoles. *Tetrahedron* **2011**, *67*, 9148–9163. [[CrossRef](#)]
32. Zubkov, F.I.; Nikitina, E.V.; Galeev, T.R.; Zaytsev, V.P.; Khrustalev, V.N.; Novikov, R.A.; Orlova, D.N.; Varlamov, A.V. General synthetic approach towards annelated 3a,6-epoxyisoindoles by tandem acylation/IMDAF reaction of furylazaheterocycles. Scope and limitations. *Tetrahedron* **2014**, *70*, 1659–1690. [[CrossRef](#)]
33. Zaytsev, V.P.; Mertsalov, D.F.; Chervyakova, L.V.; Krishna, G.; Zubkov, F.I.; Dorovatovskii, P.V.; Khrustalev, V.N.; Zarubaev, V.V. Features of oxa-bridge cleavage in hexahydro-3a,6-epoxyisoindol-1(4H)-ones: A concise method to access acetylisoindolones possessing antiviral activity. *Tetrahedron Lett.* **2019**, *60*, 151204. [[CrossRef](#)]

34. Grudova, M.V.; Gil, D.M.; Khrustalev, V.N.; Nikitina, E.V.; Sinelshchikova, A.A.; Grigoriev, M.S.; Kletskov, A.V.; Frontera, A.; Zubkov, F.I. Synthesis, X-ray characterization and theoretical study of 3a,6:7,9a-diepoxybenzo[*de*]isoquinoline derivatives: On the importance of F···O interactions. *New J. Chem.* **2020**, *44*, 20167–20180. [[CrossRef](#)]
35. Anderson, O.P.; la Cour, A.; Dodd, A.; Garrett, A.D.; Wicholas, M. Syntheses and Structures of Isoindoline Complexes of Zn(II) and Cu(II): An Unexpected Trinuclear Zn(II) Complex. *Inorg. Chem.* **2003**, *42*, 122–127. [[CrossRef](#)] [[PubMed](#)]
36. Wicholas, M.; Garrett, A.D.; Gleaves, M.; Morris, A.M.; Rehm, M.; Anderson, O.P.; la Cour, A. Size Discrimination in the Coordination Chemistry of an Isoindoline Pincer Ligand with Cd(II) and Zn(II). *Inorg. Chem.* **2006**, *45*, 5804–5811. [[CrossRef](#)]
37. SAINT-Plus, Version 7.68; Bruker AXS Inc.: Madison, WI, USA, 2007.
38. SADABS; Bruker AXS Inc.: Madison, WI, USA, 2008.
39. Sheldrick, G.M. Crystal structure refinement with SHELXL. *Acta Cryst.* **2015**, *C71*, 3–8.
40. Cowie, T.Y.; Veguillas, M.; Rae, R.L.; Rouge, M.; Zurek, J.M.; Prentice, A.W.; Paterson, M.J.; Bebbington, M.W.P. Intramolecular Nitrofuran Diels–Alder Reactions: Extremely Substituent-Tolerant Cycloadditions via Asynchronous Transition States. *J. Org. Chem.* **2017**, *82*, 6656–6670. [[CrossRef](#)] [[PubMed](#)]
41. Zaytsev, V.P.; Mertsalov, D.F.; Trunova, A.M.; Khanova, A.V.; Nikitina, E.V.; Sinelshchikova, A.A.; Grigoriev, M.S. Iodine Acetate as a Mild Selective Agent for the Wagner–Meerwein Rearrangement in 3a,6-Epoxyisoindoles. *Chem. Heterocycl. Compd.* **2020**, *56*, 930–935. [[CrossRef](#)]
42. Zaytsev, V.P.; Zubkov, F.I.; Mertsalov, D.F.; Orlova, D.N.; Sorokina, E.A.; Nikitina, E.V.; Varlamov, A.V. Continuous-flow catalytic hydrogenation of 3a,6-epoxyisoindoles. *Russ. Chem. Bull.* **2015**, *64*, 112–126. [[CrossRef](#)]
43. Rae, R.L.; Žurek, J.M.; Paterson, M.J.; Bebbington, M.W.P. Halogenation effects in intramolecular furan Diels–Alder reactions: Broad scope synthetic and computational studies. *Org. Biomol. Chem.* **2013**, *11*, 7946–7952. [[CrossRef](#)] [[PubMed](#)]
44. Berger, G.; Soubhye, J.; Wintjens, R.; Robeyns, K.; Meyer, F. Crystal packing and theoretical analysis of halogen and hydrogen-bonded hydrazone from pharmaceuticals. Evidence of type I and II halogen bonds in extended chains of dichloromethane. *Acta Crystallogr. Sect. B Struct. Sci. Cryst. Eng. Mater.* **2018**, *74*, 618–627. [[CrossRef](#)]
45. Awwadi, F.F.; Willett, R.D.; Peterson, K.A.; Twamley, B. The Nature of Halogen···Halogen Synthons: Crystallographic and Theoretical Studies. *Chem. Eur. J.* **2006**, *12*, 8952–8960. [[CrossRef](#)]
46. Metrangolo, P.; Resnati, G. Type II halogen···halogen contacts are halogen Bonds. *IUCrJ* **2014**, *1*, 5–7. [[CrossRef](#)] [[PubMed](#)]
47. Nizhnik, Y.P.; Sons, A.; Zeller, M.; Rosokha, S.V. Effects of Supramolecular Architecture on Halogen Bonding between Diiodine and Heteroaromatic N-Oxides. *Cryst. Growth Des.* **2018**, *18*, 1198. [[CrossRef](#)]
48. Bondi, A. van der Waals Volumes and Radii. *J. Phys. Chem.* **1964**, *68*, 441–451. [[CrossRef](#)]